JOURNAL OF MATERIALS SCIENCE 17 (1982) 2990–2996

Precision tensile testing of small specimens of polysulphur nitride in the scanning electron microscope

R. H. HOEL*, D. J. DINGLEY
H.H. Wills Physics Laboratory, University of Bristol, Bristol UK

Experiments have been carried out using a miniature tensometer in a scanning electron microscope to obtain high-precision mechanical tensile test data on needle-shaped crystals of $(SN)_x$. Extensions as low as 10 nm can be measured over a gauge length of varied size from a few millimetres down to a few microns. Loads were applied in a range of 0.1–10 N and measured with a sensitivity of 0.006 N. Young's modulus parallel to the chain axis of $(SN)_x$ was measured as 1.3×10^{10} N m^{-2}, the crystals yielded at 1.3×10^8 N m^{-2} at a strain of 0.9%, tensile strength was determined at 2.1×10^8 N m^{-2}.

1. Introduction

Polymeric sulphur nitride $(SN)_x$ is an unusual inorganic linear polymer which is metallic from above room temperature to about 0.3 K [1–4] where a superconducting transition is observed [5, 6]. This ranks it unique amongst polymers and was the reason for a sudden and extensive increase in research into its structure and properties. Until recently, however, there were no data available on the mechanical properties of $(SN)_x$, the reason being that the individual crystals are so small and their morphology such that testing by conventional methods is difficult.

The polymer is prepared by solid state polymerization of disulphur dinitride. The crystals develop a fibrous structure during polymerization and it is likely that not only the chain orientation, but also the presence of this fibrous texture, could strongly influence the macroscopic properties. The morphology of the crystals varies from nearly equidimensional crystals, typically a few millimetres across, to needle-shaped crystals a fraction of a millimetre thick and a few millimetres long. These crystals often grow with a twisted morphology. The needle direction coincides with the fibre direction.

Until recently, the microstructure of $(SN)_x$ was surrounded with some controversy. Studies by Hoel [7] confirmed the monoclinic structure with space group $P2_1/C$ reported by Mikulski and coworkers [8, 9]. The sulphur and nitrogen atoms polymerize to form a near planar chain of alternating *cis* and *trans* bonds, there being two such chains with four sulphur and four nitrogen atoms per unit cell (Fig. 1). The unique crystallographic *b*-axis coincides with the fibre direction and the direction of high conductivity. The chain plane is oriented within 2° of the $(\bar{1}\,0\,1)$ crystal planes.

The bond lengths along the chains are nearly equal and only slightly larger than a double bond length, so the chains are expected to be strong. The material will be less strong in other directions in the chain plane and weaker still in all directions out of the chain plane where the distances of closest approach between S–S and S–N atoms are greater than the Van der Waal distances.

Boudeulle [10] reported extensive twinning about the (1 0 0) plane in $(SN)_x$. Studies by Hoel [7] suggest at least one more twin mode, described as a 180° rotation about the reciprocal lattice direction $[\bar{1}02]$, with a mosaic spread about the chain axis of 10°. The heavy twinning is thought to be responsible for the fibrous texture of the crystals, clearly seen in scanning electron microscope images (Fig. 2).

The small size of the crystals may suggest that

*Present address: University of California, Berkeley, California, USA.

0022–2461/82/102990–07$03.34/0

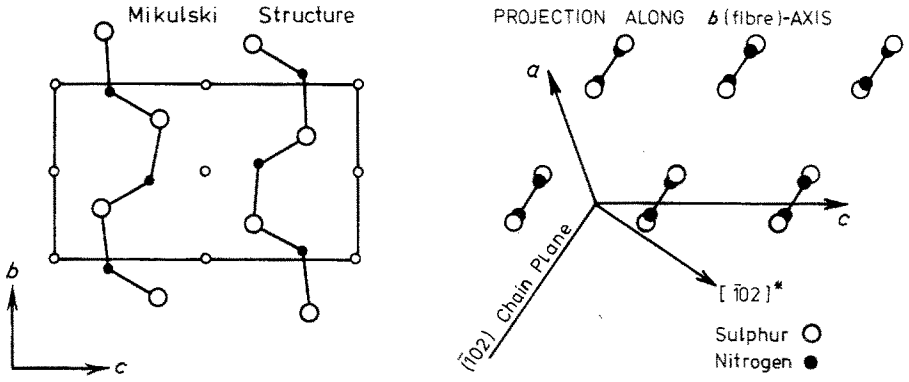

Figure 1 (1 0 0) and (0 1 0) projections of the $(SN)_x$ structure according to Mikulski.

compression tests would be easier to perform than tensile tests. The tendency of opposing faces to be non-parallel and the observed coarseness of these faces, however, complicate such tests. Measurements of Young's modulus, yield strength and fracture strength were thus determined by tensile testing using the most perfect needle-shaped crystals that could be obtained. The measurements were to be conducted using a modified "Dingley" tensometer [12] in a scanning electron microscope so that high precision in strain measurements could be achieved.

2. Experimental methods

$(SN)_x$ crystals were grown according to the method described by Mikulski *et al.* [8]. For tensile tests parallel to the fibre direction, needles with as large a length to cross-sectional dimension ratio as possible were selected.

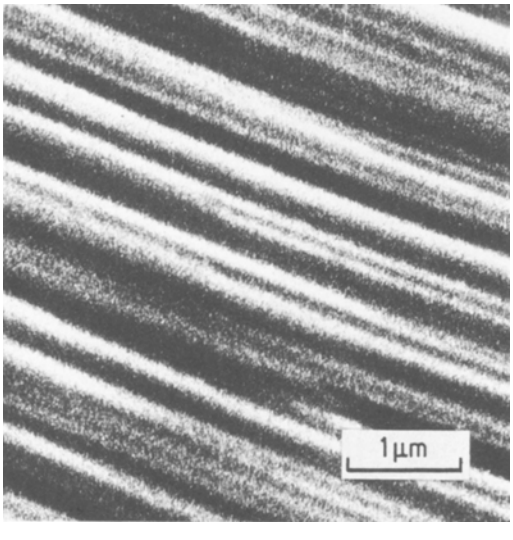

Figure 2 SEM of the bulk crystal of $(SN)_x$ illustrating the fibrous texture parallel to the needle axis.

Copper–beryllium end plates were glued to each end of the specimen using Araldite epoxy resin, as shown in Fig. 3. The crystal and the holes of the end plates were aligned under a travelling optical microscope while resting on a pair of optical glass slides. The alignment was better than 10 μm with respect to the tensile axis.

Recent experiments by Arridge *et al.* [11], on the way in which load is transferred by shear from the gripped end of a tensile specimen to its interior indicate that the stress distribution perpendicular to the direction of applied stress becomes uniform at distances from the grips typically 10–30 times the minimum cross-sectional dimension. This figure increases with the anisotropy of the crystal and is expected to be relatively high for $(SN)_x$ with its weak bonding between chains and fibrils. Thus for typical crystals 3 mm long x 0.1 mm thick, it is necessary to carry out the strain measurements on a gauge length of little more than 1 mm at the centre of the needle. Hence, the need to conduct the experiments in the SEM.

2.1. Measurements of cross-sectional area

Because typical cross-sectional dimensions were of the order of 100 μm, optical methods of measurement would give poor precision and, as interfacial angles too have to be measured, the estimated

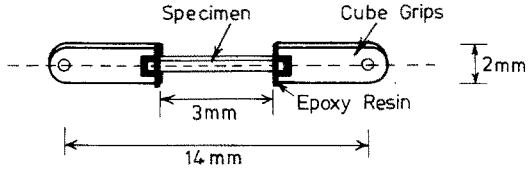

Figure 3 Illustration of end plates used to grip and align the $(SN)_x$ needles.

precision of such measurements is 50%. In the alternative method adopted, the crystal is oriented in the scanning microscope such that the needle axis is perpendicular to the electron beam and parallel to the y deflection of the scanning coils. The needle is then rotated about the needle axis and measurements made of the projected width of a crystal face on the screen or from photographs. For an initial arbitrary orientation of the needle (Fig. 4) a particular face of true width W will have a projected width

$$W_1 = W \cos \phi_1 \quad (1)$$

where ϕ_1 is as defined in the figure. Rotating the needle through a known angle θ results in a new projected width

$$W_2 = W \cos (\phi_1 + \theta). \quad (2)$$

Combining Equations 1 and 2 gives

$$W = [W_1 + \theta(W_1 \cos \theta - W_2)/\sin \theta^2]^{1/2},$$

from which the true face width W is determined. A rotation through 360° yields values for all crystal faces together with their angular separations. Accurate magnification calibration of the scanning microscope was obtained using an optical diffraction grating giving a precision of 0.1%. The precision in cross-sectional area measurements by this method for uniform specimens is typically 1%, but depends on the number of faces measured as well as on the image quality at high magnifications.

2.2. Strain measurements

Gauge lengths were also measured directly from the CRT of the scanning microscope or from photographic negatives. Irregularities on the specimen surface, as shown in Fig. 5, were often used as fiducial markers for extension measurements. In addition, a fiducial grid was evaporated onto the specimen by covering it with an electron microscope grid and coating with gold palladium. This pattern also served as an aid to check for linearity

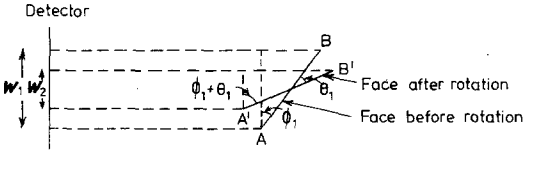

Figure 4 Sketch illustrating the method of obtaining the true width of a side face of an $(SN)_x$ needle. The projection is along the fibre axis.

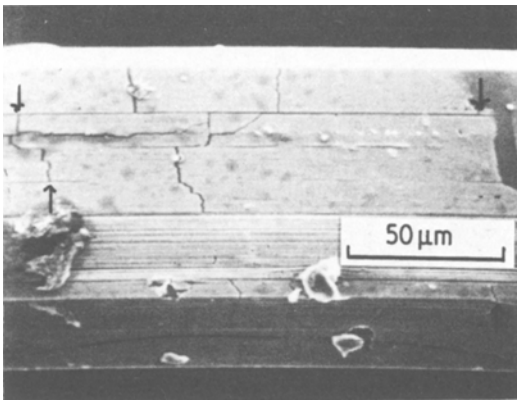

Figure 5 Irregularities on a surface of an $(SN)_x$ crystal used as fiducial markers.

in the mounting of the specimen as any non-linearity would cause distortion on loading. It was found possible to take strain measurements from a very small length of the specimen and check for strain uniformity both across and along the needle. Typically, measurements were taken from markers spaced a few microns to a few millimetres apart. Their magnified separation was typically 100 mm and it was possible to resolve a change in this length of only 0.1 m. At a magnifiction of 10^3 this corresponds to a true extension of 10 nm. This minimum detectable extension, however, depends on the resolution of the scanning image.

2.3. Load measurements

The specimens were loaded in tension using a modified "Dingley" miniature tensometer designed for applications in scanning electron microscopes [12].

Load measurement using this device is achieved as shown in Fig. 6. The specimen is stretched by the opposed motion of the two cross-heads. One end of the specimen is attached to its cross-head via a [-shaped grip. The grip, in turn, presses against a pin passing through the cross-head which

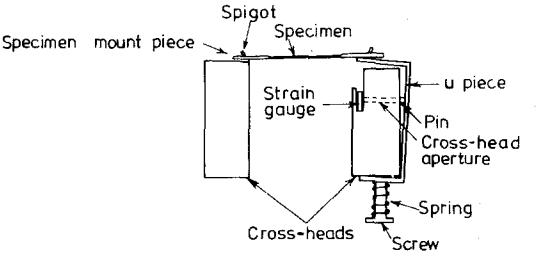

Figure 6 Illustration of load-measuring system in the Dingley tensometer.

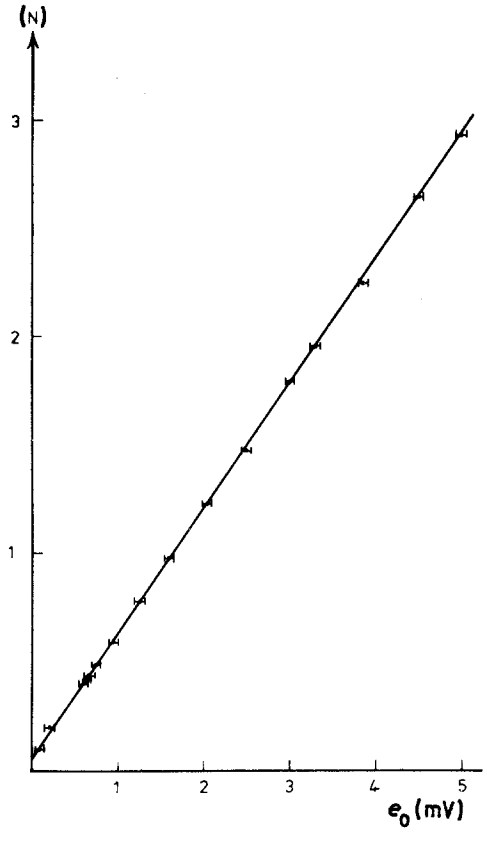

Figure 7 Calibration curve for load cell of Dingley tensometer.

forces a Cu–Be spring to bend. A strain gauge glued to the spring measures the amount of bend. This was found to be directly proportional to the applied load as can be seen from the calibration curve in Fig. 7. The voltage signal plotted in this graph is the out-of-balance signal of a Wheatstone bridge network of which the strain gauge is one branch. The sensitivity of the load cell may be increased by either decreasing the stiffness of the Cu–Be spring, or increasing the length of the [-piece lever. Using a standard constant voltage supply and digital voltmeter of better than 10 μV sensitivity, a load resolution of $\pm$ 0.04 N can be achieved.

3. Results

Specimens were carefully selected according to uniformity in cross-sectional dimensions and untwisted morphology.

Two crystals of sufficient quality were tested. Their cross-sectional shapes are sketched in Fig. 8 and the cross-sectional areas were, respectively, 1.05×10^{-8} μm^2 ($\pm$ 5%) and 4.52×10^{-9} μm^2 ($\pm$ 5%). The rather large 5% uncertainty in cross-sectional area is due to a non-uniformity in cross-sectional dimensions along the specimen length. The load–strain curves obtained for these crystals are shown in Fig. 9, and in Table I are listed the values obtained for their mechanical properties. The average value for Young's modulus was 1.3×10^{10} N m^{-2}, the material yielded at an average stress of 1.3×10^{8} N m^{-2} and at a strain of 0.9%. The average tensile strength was 2.1×10^{8} N m^{-2}.

Fig. 10 shows a scanning micrograph of a fractured surface revealing the highly fibrous nature of the material. Transmission electron microscopy of individual fibres shows them to consist of numerous small multiply twinned crystals [7]. An electron diffraction pattern from the deformed fibre in Fig. 11a is shown in Fig. 11b. The fibre axis is vertical, so the horizontal streaking is due to reciprocal lattice extensions in this direction. If the crystal planes parallel to the fibre axis had been bent uniformly with the fibre, then the diffraction spots should show additional streaking parallel to the curvature. Instead, discrete spots are seen in this direction, indicating that the fibre kinks rather than bends. The plastic flow that has occurred after yield in Fig. 9 is, therefore, unlikely to be due to shear of the fibres themselves, but rather to inter-fibre sliding.

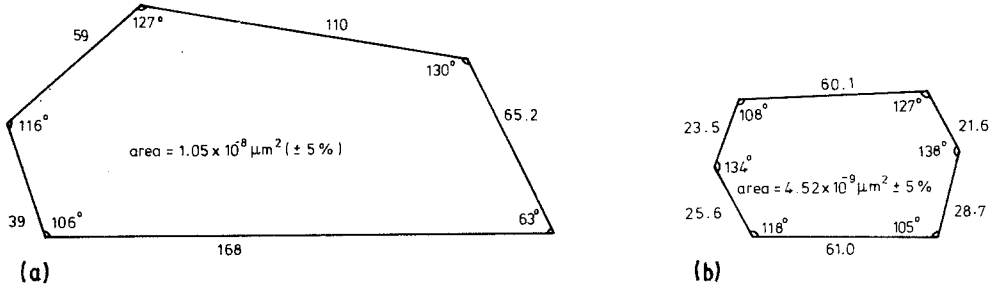

Figure 8 Cross-sectional dimensions of two $(SN)_x$ needles. Dimensions in μm.

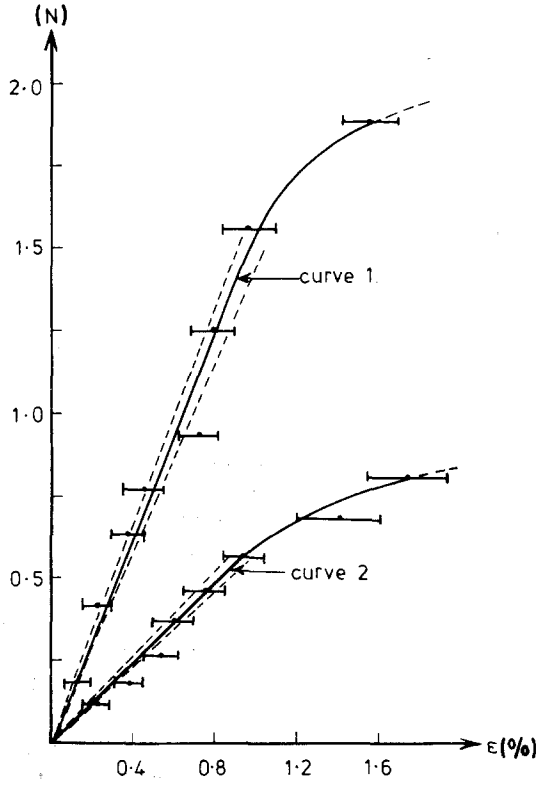

Figure 9 Load strain curves of two $(SN)_x$ needles.

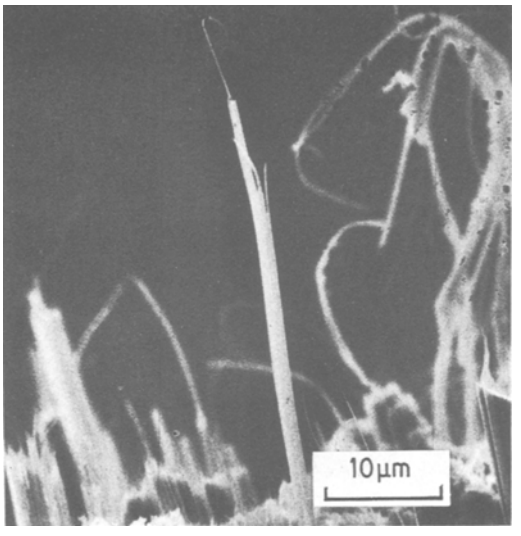

Figure 10 SEM image of fracture surface of $(SN)_x$.

4. Discussion

Earlier experiments on $(SN)_x$ by Davidson and Yoffe [13], and Brown and Chiang [14] resulted in the mechanical test data shown in Table II. Davidson and Yoffe used a Marsh Micro Testing Machine [15], where the load is applied to the specimen by a torsion balance. Cross-sectional dimensions were measured optically. The device is applicable to thin whiskers of 1–75 μm cross-sectional dimensions and typically 1 mm length so that Davidson and Yoffe had to cut whiskers from the bulk crystals with the aid of a needle. Brown and Chiang did compression tests using an Instron machine. The difficulties encountered using this method arise from the lack of flatness of the crystals and the problems of measuring yield stress and tensile strength accurately due to buckling of the specimens.

An estimate of the uncertainty in cross-sectional area measured optically in the Davidson–Yoffe experiment is 20%. Brown and Chiang quote a 10% uncertainty in their cross-sectional area measurements plus 20% in gauge length and 2% in load. The precision of these experiments is thus considerably worse than in the present case. It is seen, however, that there is good general agreement between the various experiments in the values obtained for Young's modulus. The wider range of values obtained by Davidson and Yoffe can be ascribed to the variation in quality of their cut specimens. There is good agreement between the present authors and Davidson and Yoffe in the values for the yield strength and tensile strength. The low value in tensile strength obtained by Brown and Chiang may be due to the particular difficulty in determining this parameter by compression tests. There is, however, a significant difference in the yield strains obtained by the present authors and Davidson–Yoffe. This may arise from the way in which Davidson–Yoffe define the yield point on their stress–strain curve. It is possible, however, that it results from the differences in crystal-growth procedures, which for $(SN)_x$ are by no means straightforward.

When we compare our mechanical test data

TABLE I Mechanical properties for two $(SN)_x$ crystals obtained from the load–extension curves in Fig. 9

	Young's modulus ($\times 10^{10}$ N m^{-2})	Yield stress ($\times 10^{8}$ N m^{-2})	Yield strain (%)	Tensile stress ($\times 10^{8}$ N m^{-2})
Crystal 1	1.28 ± 0.13	1.50 ± 0.1	1.0 ± 0.1	1.98 ± 0.14
Crystal 2	1.35 ± 0.14	1.15 ± 0.15	0.8 ± 0.1	2.15 ± 0.15

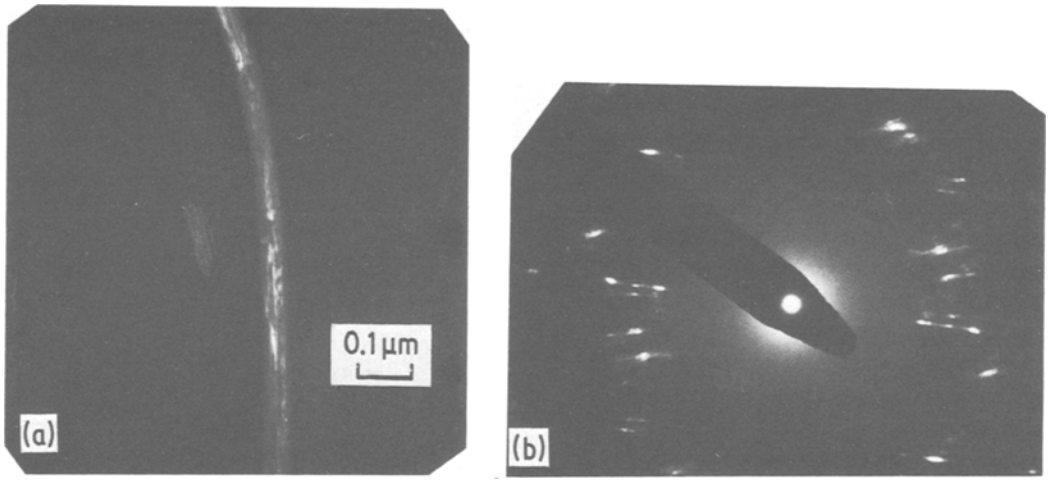

Figure 11 (a) Dark-field TEM-image of bent $(SN)_x$ fibre. (b) Corresponding electron diffraction pattern.

with other materials, we find the yield strength of 13×10^7 N m^{-2}, greater than that of most linear polymers ($1.4–8.0 \times 10^7$ N m^{-2}) whilst the tensile strength of 2.1×10^8 N m^{-2} is very similar to values for other oriented polymer fibres such as cellulose acetate, polyethylene and nylon whose tensile strengths are 1.7, 4.8 and 6.4×10^8 N m^{-2}, respectively. These values are also similar to those of most metals (e.g. 8×10^7 N m^{-2} for aluminium and 6×10^8 N m^{-2} for stainless steel). However, the value for Young's modulus of $(SN)_x$, 1.3×10^{10} N m^{-2}, is considerably less than that of most metals $2–7 \times 10^{11}$ N m^{-2}) but about 30 times the value for high-density polyethylene.

Conclusions

It has been shown that precise values for the mechanical properties of small brittle and fibrous needles of irregular cross-sectional shape can be obtained by conducting the measurements in a scanning electron microscope. Values obtained for our $(SN)_x$ crystals in the direction of the chain axis, i.e., that in which they exhibit metallic character, show that they were 50 times less stiff than metals, but had approximately the same breaking strength of a metal such as aluminium. They exhibited a small amount of plasticity which is believed to be a result of inter-fibre sliding rather than shear of the fibres themselves.

Acknowledgements

The authors thank Drs J. Stejny, P. Barnett and R. Trinder for supplying $(SN)_x$ crystals, and the Norwegian body "Statens Lanekasse" for providing the financial support.

References

1. V. V. WALATKA, Jr, M. M. LABES and J. H. PERLSTEIN, *Phys. Rev. Lett.* **31** (1973) 1139.
2. C. HSU and M. M. LABES, *J. Chem. Phys.* **61** (1974) 464.
3. A. A. BRIGHT, M. J. COHEN, A. F. GAVITO, A. J. HEEGER, C. M. MIKULSKI and A. G. MacDIARMID, *Appl. Phys. Lett.* **26** (1975) 612.
4. G. B. STREET, H. ARNAL, W. D. GILL, P. M. GRANT and R. L. GREEN, *Mat. Res. Bull.* **10** (1975) 877.
5. R. L. GREEN, G. B. STREET and L. J. SUTER, *Phys. Rev. Lett.* **34** (1975) 57.
6. A. A. BRIGHT, M. J. COHEN, A. F. GAVITO, A. J. HEEGER, C. M. MIKULSKI, P. J. RUSSO and A. G. MacDIARMID, *ibid* **34** (1975) 206.

TABLE II Mean values for mechanical properties of $(SN)_x$ obtained by different authors

	Young's modulus ($\times 10^{10}$ N m^{-2})	Yield strength ($\times 10^7$ N m^{-2})	Yield strain (%)	Tensile strength ($\times 10^7$ N m^{-2})
Hoel and Dingley [7, 12]	1.15–1.49	10–16	0.7–1.1	18.4–23.0
Davidson and Yoffe [13]	1.13–3.09	4.68–14.50	0.39–0.54	5.50–36.60
Brown and Chaing [14]	1.0–3.1			1.5–7.4

7. R. H. HOEL, Ph.D. Thesis, University of Bristol (1979).
8. C. M. MIKULSKI, P. J. RUSSO, M. S. SARAN, A. G. MacDIARMID, A. F. GAVITO and A. J. HEEGER, *J. Amer. Chem. Soc.* **97** (1975) 6358.
9. M. J. COHEN, A. F. GAVITO, A. J. HEEGER, A. G. MacDIARMID, C. M. MIKULSKI, M. S. MORAN and J. KLEPPINGER, *ibid.* **98** (1976) 3844.
10. M. BOUDEULLE, Ph.D. Thesis, University of Lyon (1974).
11. R. G. C. ARRIDGE, P. J. BARHAM, C. J. FARREL and A. KELLER, *J. Mater. Sci.* **11** (1976) 1978.
12. D. J. DINGLEY, *Micron* **1** (1969) 206.
13. A. T. DAVIDSON and A. D. YOFFE, *Phil. Mag.* **36** (1977) 1083.
14. N. BROWN and C. K. CHIANG, *J. Mater. Sci.* **14** (1979) 49.
15. D. M. MARSH, *J. Sci. Instrum.* **38** (1961) 229.

Received 2 April 1981
and accepted 22 March 1982